Chirality– and thickness-dependent thermal conductivity of few-layer graphene: a molecular dynamics study

Wei-Rong Zhong[1], Mao-Ping Zhang[1], Bao-Quan Ai[2*] and Dong-Qin Zheng[1]

[1]*Department of Physics and Siyuan Laboratory, College of Science and Engineering,*
Jinan University, Guangzhou 510632, P. R. China and

[2]*Laboratory of Quantum Information Technology, ICMP and SPTE,*
South China Normal University, Guangzhou, 510006 P. R. China
(Dated: November 1, 2018)

Abstract

The thermal conductivity of graphene nanoribbons (layer from 1 to 8 atomic planes) is investigated by using the nonequilibrium molecular dynamics method. We present that the room-temperature thermal conductivity decays monotonically with the number of the layers in few-layer graphene. The superiority of zigzag graphene in thermal conductivity is only available in high temperature region and disappears in multi-layer case. It is explained that the phonon spectral shrink in high frequency induces the change of thermal conductivity. It is also reported that single-layer graphene has better ballistic transport property than the multi-layer graphene.

In the past decade, more and more attentions have been given to the question of what happens with thermal conductivity when goes to low-dimensional materials [1]. A two-dimensional materials-graphene [2], in addition to its exceptional electric [3] and optical properties [4], [5], reveals unique high thermal conductivity. Thermal conductivity of single-layer graphene as well as of carbon nanotubes is dependent on the chirality [6]. Recent theoretical studies suggest that the thermal conductivity of single-layer zigzag graphene is 20-50% larger than that of the single-layer armchair graphene [7]. However, whether the superior thermal conductivity of zigzag graphene remains available for multi-layer graphene has not got enough attention and concern.

Additionally, experimental demonstrations have shown that the thermal conductivity gets a decrease at the two- to three-dimensional (2D to 3D) crossover of few-layer graphene [8]. The fact that the thermal conductivity of large enough graphene sheets should be higher than that of basal planes of bulk graphite was predicted theoretically by Klemens [9]. Generally, thermal transport in conventional thin films still retains 'bulk' features because the cross-sections of these structures are measured in many atomic layers. Heat conduction in such nanostructures is dominated by extrinsic effects, for example, phonon-boundary or phonon-defect scattering [10]. A recent experimental observation of high-quality few-layer graphene materials shows that the room-temperature thermal conductivity changes from ~2,800 to ~1,300 $Wm^{-1}K^{-1}$ when the number of atomic planes in few-layer graphene increases from 2 to 4. It is explained that the observed evolution from two dimensions to bulk attributed to the cross-plane coupling of the low-energy phonons and changes in the phonon Umklapp scattering [8].

Recently, the method of molecular dynamics simulation has been successful in discovering thermal conductivity and thermal rectification of the nanostructures [7],

[11]. This method, which builds the system from the bottom up, is useful to understand the intrinsic behavior, i.e., the phonon spectral behavior behind the significant change of a material's ability to conduct heat [12]. In this paper, we will study the thermal conductivity of graphene ribbons (layer from 1 to 8 atomic planes) by using the nonequilibrium molecular dynamics method. By investigating the thermal conductivity and the phonon spectral behavior of multi-layer graphene, we try to reveal the coupling of the low-energy phonons from a more fundamental principle. The obtained results are of significance for understanding the thermal properties in low-dimensional materials and may open up few-layer graphene applications in the nanoscale thermal device such as thermal diode [13], thermal transistor [14] and so on.

In our simulations, we have used classical molecular dynamics method based on the Tersoff-Brenner potential [15] of C-C bonding interactions. The equations of motion for atoms in either the left or right Nosé-Hoover thermostat are [7], [16]

$$\frac{d}{dt}p_i = F_i - \Gamma p_i; \frac{d}{dt}\Gamma = \frac{1}{Q}\left[\sum_i \frac{p_i^2}{2m_i} - 3Nk_BT_0/2\right],$$
(1)

where p_i is the momentum and F_i is the force applied on the i-th atom. $Q = 3Nk_BT_0\tau^2/2$, where τ is the relaxation time, which is kept as $1ps$. Γ is the dynamic parameter of the thermostat, $T(t)$, which is defined as $\frac{m_i}{3k_B}(vx(t)^2 + vy(t)^2 + vz(t)^2)$, where $v(t)$ is the time-dependent velocity, is the instant temperature of the heat baths at time t. T_0 (T_L or T_R). The set temperature of the heat baths, are placed in the two ends of the graphene and the temperature difference is denoted as $\Delta T = T_L - T_R$. For the convenience of comparison, here we set $T_L = 350K, T_R = 300K$, which are near the room temperature. In order to avoid the spurious global rotation of the graphene in the simulation, we use fixed boundary condi-

tion in the two ends of the graphene. The fixed region and the heat baths occupy one layer and six layers of atoms respectively. N is the number of the atoms in the heat baths, k_B is the Boltzmann constant and m is the mass of the carbon atom.

We integrate these equations of motion by a Verlet method [17]. The time step is $0.55\ fs$, and the simulation runs for 1×10^8 time steps giving a total molecular dynamics time of $55\ ns$. Generally, $T(t)$ can stabilize around the set value T_0 after 2 ns for single-layer graphene and 20 ns for four-layer graphene. Time averaging of the temperature and heat current is performed from 35 to 55 ns. The heat bath acts on the particle with a force $-\Gamma p_i$; thus the power of heat bath is $-\Gamma p_i^2/m$, which can also be regarded as the heat flux come out of the high temperature heat bath and injected into the low temperature heat bath. The total heat flux injected from the heat bath to the system can be obtained by $J = \sum_i [-\Gamma p_i^2/m_i] = -3\Gamma N k_B T(t)$, where the subscript i runs over all the particles in the thermostat [16]. The final thermal conductivity is calculated from the well-known Fourier's law $\kappa = Jl/(\Delta T whn)$, in which l, w, and h (=0.335nm) are the length, width and thickness of each layer graphene, respectively. n is the number of the atomic planes.

In Fig. 1, we explicitly observed the decrease of thermal conductivity as the number of layers changes from 1 to 8. This change implies a crossover from 2D graphene to 3D graphite. For the single-layer graphene, the room-temperature thermal conductivity of zigzag nanoribbons is 2276 $\mathrm{Wm^{-1}K^{-1}}$, which is 43% larger than that of armchair nanoribbons. From the inset of Fig. 1, one can find that this attenuation relationship is not qualitatively varied with the graphene ribbon width. Another interesting phenomenon, that the zigzag graphene loses its superiority in thermal conductivity as the number of layers increases to 5, predicts that the chirality dependence of thermal conductivity may disappear for 3D graphite. Here we have to point out that the superiority in thermal conductivity of zigzag nanoribbons is only available for the temperature larger than 220K. When the temperature is less than 220K, as displayed in Fig. 2, we can observe that armchair graphene has better thermal conductivity than zigzag graphene. The temperature-dependent thermal conductivity of armchair and zigzag graphene can be interpreted by the number of phonons and the path for phonons passing. From the structure of armchair and zigzag graphene, we can know that the path in armchair graphene $(1.35l)$ is longer than that $(1.15l)$ in zigzag graphene with the same length, where l is the length of graphene. Similarly, at the same width, the armchair graphene occupies more areas and particles than the zigzag graphene (the ratio is about 1.15). At high temperature, longer path means more phonons scattering. At low temperature, more particles mean more phonons to conduct heat. Therefore, the thermal conductivity of armchair is larger at low temperature and smaller at high tem-
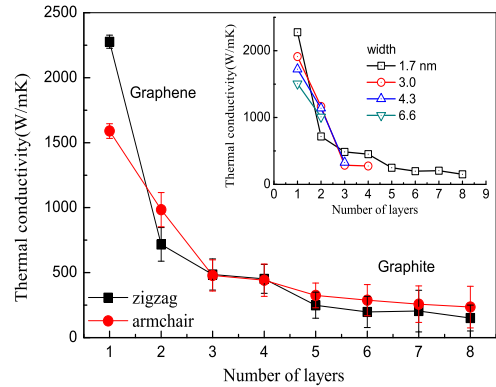
perature than that of the zigzag graphene.

FIG. 1: Layer-dependent thermal conductivity of few-layer graphene. The 1-layer nanoribbons refer to graphene and the 5~8 layers nanoribbons are similar to utra-thin graphite. The inset is the layer-dependent thermal conductivity for various width zigzag graphene. The average temperature is 325K.
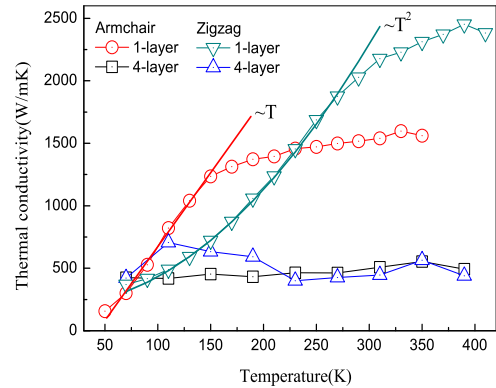

FIG. 2: Temperature dependence of thermal conductivity of zigzag and armchair graphene for one and four layers atomic planes.

Recent experiments suggest that thermal transport at the nanoscale is dominated by a ballistic rather than a diffusive mechanism [18]. For the single-layer graphene, figure 3 illustrates that thermal conduction at low temperature is dominated by the straight or bending mode, with a power law of ~T for armchair graphene and ~T^2 for zigzag graphene. The former is good agreement with the elastic-shell-based theoretical results in graphene with finite width [19]. The later shows that the chirality can change the power law relationship between the thermal conductivity and the temperature. We explained that the difference between the power law thermal conductivity of armchair and

zigzag graphenes is mainly due to the different phonon scattering rates at the armchair and zigzag edges [7]. This power law relationship implies that the graphene conduct heat mainly through ballistic transport mode in this temperature region [19].

For the multi-layer graphene, the ballistic transport decays at the same temperature region and the thermal conductivity fluctuates near 500 Wm^{-1}K^{-1}. The crossover from 2D graphene to 3D graphite, which induces the decrease of thermal conductivity of few-layer graphene, has been explained as the cross-plane coupling of the low-energy phonons and changes in the phonon Umklapp scattering [8]. For the single-layer graphene, i.e., in the absence of cross-planes coupling, the thermal transport mode is of ballistic. Ballistic transport means less collision of phonons, however in the presence of cross-planes coupling, the phonons will scatters with the particles at the interface between the layers and then the thermal conductivity will decrease. Therefore, it is reasonable that the cross-plane coupling, which is similar to the inter-chain coupling in double Frenkel-Kontorova chains [20], will result in a suppression of thermal conductivity in graphene nanoribbons. Here, from the view of spatially-resolved phonon spectral behavior shown in Figs. 3(a) and (b), we present that the phonon occupies a wide frequency region for monolayer graphene in the absence of layer-to-layer coupling. However, for four-layer graphene, in the presence of layer-to-layer coupling, as shown in Figs. 3(c) and (d) the phonons in high frequency region from 1,200 to 1,600 cm^{-1} shrinks and weakens at the edge of nanoribbons. In Refs. [12] and [21], the results about carbon nanotubes and graphenes have illustrated that the high frequency phonon modes, which can be affected by the edge sensitively, play a major role in the low-dimensional non-Fourier heat conduction. Obviously, the cross-planes coupling can induce unperfect and rough edges in the graphene. The edge roughness can suppress thermal conductivity strongly [12]. Thus, as the high frequency phonons shrinks with the layer-to-layer coupling, the material's ability to conduct heat will decay.

In summary, the thermal conductivity of few-layer graphene strongly depends on the number of atomic planes. The reduction of the ability of few-layer graphene to conduct heat is attributed to the crossover from 2D graphene to 3D graphite. We speculated this decreasing evolution in thermal conductivity is mainly due to the shrinking of high frequency phonon induced by the cross-layer coupling. We obtained the thermal conductance of zigzag and armchair nanoribbons as a power law relationship of the temperature at low temperature. For the multi-layer graphene, the thermal conductivity is independent on the chirality. Although our calculations indeed show that the number of layer is disadvantageous to the thermal conductivity in few-layer graphene, the intriguing questions about the thermal conductivity of few-layer graphene are expected to stimulate further experimental and theoretical investigations of phonon transport.
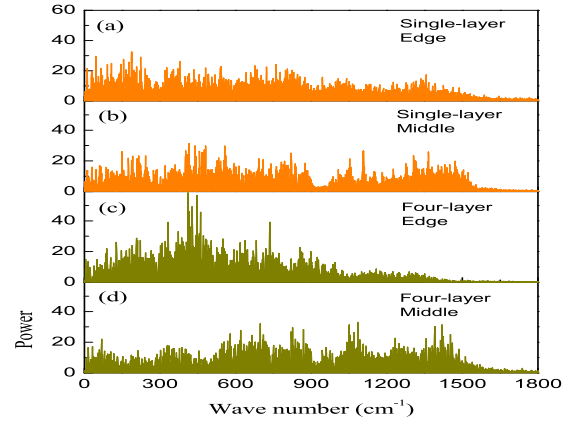

FIG. 3: Spatially-resolved phonon spectrum in the zigzag graphene. Edge (a) and middle (b) particle in the single-layer graphene, edge (c) and middle (d) particle in the four-layer graphene. The parameters are $T_L = 350K$, $T_R = 300K$.

* Electronic address: wrzhong@hotmail.com, aibq@scnu.edu.cn
[1] S. Lepri, R. Livi, and A. Politi, Phys. Rep. **377**, 1 (2003).
[2] K. S. Novoselov, A. K. Geim, S. V. Morozov, D. Jiang, Y. Zhang, S. V. Dubonos, I. V. Grigorieva and A. A. Firsov, Science, **306**, 666-669 (2004).
[3] Y. B. Zhang, Y. W. Tan, H. L. Stormer, and P. Kim, Nature, **438**, 201 204 (2005).
[4] R. R. Nair, P. Blake, A. N. Grigorenko, K. S. Novoselov, T. J. Booth, T. Stauber, N. M. R. Peres and A. K. Geim, Science, **320**, 1308 (2008).
[5] A. A. Balandin, S. Ghosh, W. Bao, I. Calizo, D. Teweldebrhan, F. Miao, C. N. Lau, Nano Lett. **8**, 902 907 (2008).
[6] W. Zhang, Z. Zhu, F. Wang, T. Wang, Litao Sun and Z. Wang, Nanotechnology, **15**, 936–939 (2004).
[7] J. Hu, X. Ruan, and Y. P. Chen, Nano Lett., **9**, 2730-2735 (2009).
[8] S. Ghosh, W. Bao, D. L. Nika, S. Subrina, E. P. Pokatilov, C. N. Lau and A. A. Balandin, Nature Material, **9,** 555 (2010).
[9] P. G. Klemens, J. W. Bandgap Mater. **7**, 332 339 (2000).
[10] A. I. Hochbaum, R. Chen, R. D. Delgado, W. Liang, E. C. Garnett, M. Najarian, A. Majumdar, P. Yang, Nature, **451**, 163 167 (2008).
[11] G. Wu and B. Li, J. Phys.: Condens. Matter, **20,** 175211 (2008).
[12] A. V. Savin, Y. S. Kivshar, and B. Hu, Phys. Rev. B, **82**, 195422 (2010).
[13] C. W. Chang, D. Okawa, A. Majumdar, and A. Zell, Science 314, 1121 (2006).

[14] B. Li, Lei Wang, and Giulio Casati, Appl. Phys. Lett. **88**, 143501 (2006).

[15] D. W. Brenner, Phys. Rev. B **42**, 9458 (1990).

[16] G. Wu and B. Li, Phys. Rev. B **76**, 085424 (2007).

[17] H. Rafii-Tabar, Computational Physics of Carbon Nanotubes, Cambridge University Press, New York (2008).

[18] S. Ghosh, I. Calizo, D. Teweldebrhan, E. P. Pokatilov, D. L. Nika, A. A. Balandin, W. Bao, F. Miao, C. N. Lau, Appl. Phys. Lett., **92**, 151911 (2008).

[19] E. Munoz, J. Lu, and B. I. Yakobson, Nano Lett., **10**, 1652–1656 (2010).

[20] W. R. Zhong, Phys. Rev. E **81**, 061131 (2010).

[21] J. Shiomi and S. Maruyama, Phys. Rev. B 73, 205420 (2006).